Overview of the Space Launch System Ascent Aeroacoustic Environment Test Program

Andrew J. Herron[1], William A. Crosby[2], and Darren K. Reed[3]
NASA George C. Marshall Space Flight Center, Huntsville Alabama, 35812

Characterization of accurate flight vehicle unsteady aerodynamics is critical for component and secondary structure vibroacoustic design. The Aerosciences Branch at the National Aeronautics and Space Administration (NASA) Marshall Space Flight Center has conducted a test at the NASA Ames Research Center (ARC) Unitary Plan Wind Tunnels (UPWT) to determine such ascent aeroacoustic environments for the Space Launch System (SLS). Surface static pressure measurements were also collected to aid in determination of local environments for venting, CFD substantiation, and calibration of the flush air data system located on the launch abort system. Additionally, this test supported a NASA Engineering and Safety Center study of alternate booster nose caps. Testing occurred during two test campaigns: August – September 2013 and December 2013 – January 2014. Four primary model configurations were tested for ascent aeroacoustic environment definition. The SLS Block 1 vehicle was represented by a 2.5% full stack model and a 4% truncated model. Preliminary Block 1B payload and manned configurations were also tested, using 2.5% full stack and 4% truncated models respectively. This test utilized the 11 x 11 foot transonic and 9 x 7 foot supersonic tunnel sections at the ARC UPWT to collect data from Mach 0.7 through 2.5 at various total angles of attack. SLS Block 1 design environments were developed primarily using these data. SLS Block 1B preliminary environments have also been prepared using these data. This paper discusses the test and analysis methodology utilized, with a focus on the unsteady data collection and processing.

Nomenclature

AAT	=	SLS Ascent Aeroacoustic Wind Tunnel Test
AMO	=	acoustic mitigation option
ARC	=	NASA Ames Research Center
BMO	=	buffet mitigation option
BSM	=	booster separation motor
CFD	=	computational fluid dynamics
dB	=	decibels referenced to 20×10^{-6} Pa
DSC	=	data system coordinator
ES	=	engine section
ESM	=	Encapsulated Service Module
ESP	=	electronically scanned pressure
EUS	=	Exploration Upper Stage
EV33	=	MSFC Aerosciences Branch
f	=	frequency
FADS	=	Flush Air Data System
FPL	=	fluctuating pressure level
ICPS	=	Interim Cryogenic Propulsion Stage
l	=	characteristic length
LaRC	=	NASA Langley Research Center
LAS	=	Launch Abort System

[1] Aerospace Engineer, Aerosciences Branch, EV33.
[2] Aerospace Engineer, Aerosciences Branch, Jacobs ESSSA Group.
[3] Aerospace Engineer, Fluid Dynamics Branch, ER42.

LH2 = liquid hydrogen
LOX = liquid oxygen
$L_{p,MS}$ = model scale narrowband FPL
LVSA = Launch Vehicle Stage Adapter
MPCV = Multi-Purpose Crew Vehicle
MSA = MPCV Stage Adapter
MSFC = NASA Marshall Space Flight Center
NESC = NASA Engineering and Safety Center
OAFPL = overall FPL
OML = outer mold line
P_{ref} = reference pressure
p'_{rms} = root-mean-square acoustic pressure
PSD = power spectral density
q_∞ = free stream dynamic pressure
RBOS = retro-reflective background oriented schlieren
SLS = Space Launch Sytem
SRB = solid rocket booster
St = Strouhal number
SWT = UPWT Supersonic Wind Tunnel
T = static temperature
TWT = UPWT Transonic Wind Tunnel
U = flow velocity
UPWT = ARC Unitary Plan Wind Tunnels
USA = Upper Stage Adapter
α = angle of attack
α_T = total angle of attack, $(\alpha^2+ \beta^2)^{1/2}$
β = sideslip angle
$\Delta C'_p$ = nondimensional FPL coefficient
Φ_{sc} = structural coordinate system clocking angle

Notice to Readers

The predicted performance and certain other features and characteristics of the Space Launch System vehicle are defined by the U.S. Government to be Sensitive But Unclassified (SBU). Therefore, values in plots and figures have been either removed or normalized to arbitrary values.

I. Introduction

CHARACTERIZATION of accurate flight vehicle unsteady aerodynamics is critical for component and secondary structure vibroacoustic design and qualification. Empirical methods exist to attempt prediction of external fluctuating pressure levels (FPLs) induced during vehicle ascent. However, the uncertainty of such methods can result in either an under-conservative or over-conservative design. Neither of these outcomes is desirable. Scaling wind tunnel and flight data from similar launch vehicles or protuberances generally yields better results, but is still laden with undesirable uncertainty and therefore risk. Computational fluid dynamics (CFD) is making great strides in the area of unsteady aerodynamics, but is at present too computationally expensive to determine vehicle-wide environments across the frequency range of interest. As a result, performing a large-scale wind tunnel test is still the best method for developing vehicle zonal and protuberance ascent aeroacoustic environments[1].

To satisfy this need for the Space Launch System (SLS) program, the Aerosciences Branch (EV33) at the NASA Marshall Space Flight Center (MSFC) conducted the SLS Ascent Aeroacoustic Wind Tunnel Test (AAT) program in the NASA Ames Research Center (ARC) Unitary Plan Wind Tunnels (UPWT) to obtain aeroacoustic pressure measurements on several SLS scaled vehicle configurations. The test data were used to determine aeroacoustic environments of the SLS configurations during the ascent phase of flight.

Several secondary objectives were included as well. Surface static pressure measurements were made to aid in providing local environments for venting, CFD substantiation, and calibration of the Orion Multi-Purpose Crew Vehicle (MPCV) Launch Abort System (LAS) Flush Air Data System (FADS). An effort was also included to examine the effects of alternate booster nose caps for potential use with advanced booster designs in support of a request by the NASA Engineering and Safety Center (NESC)[2]. Additional model variations were tested to determine

their effectiveness as buffet and acoustic mitigation options (BMOs and AMOs). The potential need for these mitigation options arose from buffet and aeroacoustic pressure level magnitudes in the area of the solid rocket booster (SRB) forward attach point observed during the 2012 SLS Transonic Buffet Environment Test Program[3].

Facility test numbers describing these tests are T11-0265, T97-0266, T11-0273, and T97-0274[4,5]. Data were obtained at Mach numbers from 0.7 to 1.4 in the 11' x 11' Transonic Wind Tunnel (TWT) and from 1.55 to 2.5 in the 9' x 7' Supersonic Wind Tunnel (SWT). Angle of attack (α) and sideslip angle (β) were varied from -6° to +6°. A nominal Reynolds number of 3-million per foot was primarily tested, although limited data were also obtained at 5-million per foot to assess data sensitivity to Reynolds number. For the first test campaign[4], models representing the SLS Block 1 and Block 1B vehicles were used, with additional variations representing the NESC nose caps and BMO flow fences mounted to the core intertank. A second test campaign[5] was conducted to satisfy changing programmatic needs and challenges and to explore additional BMOs and also AMOs. These included variations on the core mounted flow fences examined during the first test campaign, and added booster mounted flow fences and several fairings intended to change the shape of the SRB forward attach hardware. Additionally, data were collected for the baseline SLS Block 1 configuration for validating reliability to the first test campaign and also to further populate the test matrix to aid in defining the vehicle aeroacoustic environments in response to a new programmatic total angle of attack (α_T) limit.

Installation in the first campaign began on 19 August 2013 in the TWT with the full stack version of the SLS Block 1 test article. The first air-on period occurred on 20 August. A total of 573 runs, consisting of 3,047 data points, were obtained after completion of all configurations tested in the TWT. Transition to the SWT began on 29 August, immediately following the conclusion of testing in the TWT. Initial runs were collected with the full stack version of the SLS Block 1 configuration in the SWT beginning on 30 August. SWT testing concluded 5 September with a total of 223 runs, consisting of 1,151 data points. A total of 220.17 occupancy hours were accumulated for the test program. Two shift operations (3rd and 1st) prevailed during the course of testing.

Installation for the second campaign began 13 December 2013 in the TWT with the first air-on period occurring on 17 December. A total of 254 runs, consisting of 555 data points, were obtained after completion of all configurations tested in the TWT. Transition to the SWT began on 2 January 2014. Initial runs were collected on 7 January. Testing concluded 8 January with a total of 117 runs consisting of 319 data points. A total of 92.3 occupancy hours were accumulated for the test program conducted in single (1st) shift operations.

II. SLS Vehicle and Modeling

A. SLS Vehicle Description

The SLS is an evolvable vehicle system consisting of a payload section, upper stage, and common core aided by two 5-segment SRBs. For the SLS-10003 Block 1 configuration, the payload section is made up of the LAS tower and MPCV. The MPCV Stage Adapter (MSA) transitions the MPCV Encapsulated Service Module (ESM) to the Interim Cryogenic Propulsion Stage (ICPS) upper stage. The ICPS transitions to the liquid oxygen (LOX) tank forward skirt via the Launch Vehicle Stage Adapter (LVSA). The SLS-27000 and -28000 Block 1B configurations replace the LVSA with a cylindrical interstage and the ICPS with the Exploration Upper Stage (EUS). The SLS-27000 Block 1B cargo variant tops the EUS with an ogive payload fairing. The SLS-28000 Block 1B crew variant tops the EUS with an Upper Stage Adapter (USA) and MPCV with LAS. For all configurations, the core consists of LOX tank and liquid hydrogen (LH2) tanks separated by an intertank. The engine section (ES) with four RS-25 engines are at the base of the LH2 tank. The left and right SRBs attach at the intertank and ES. Both SRBs consist of five solid fuel segments capped with a cylindrical forward skirt and conical nose. A conical aft skirt and nozzle is downstream of the aft fuel segment. The SRB attach hardware on the SRB side is at the booster forward skirt and around the aft fuel segment via an external attach ring.

B. SLS AAT Model

The AAT utilized newly fabricated models of two different scales representing the SLS ascent configuration based on the outer mold lines (OMLs) established in July 2012, with some slight variances from subsequent vehicle updates. Full stack models at 2.5%-scale represented the SLS-10003 and -27000 configurations. In addition, 4%-scale models were tested representing truncated versions of the SLS-10003 and -28000 configurations. The vehicle station for truncation was equivalent to the SRB nose tips. Therefore, only the center body was modeled in the truncated models. The SLS-10004 configuration OML was established in time to influence some modeled protuberance changes, including core stage systems tunnel, core stage LOX feedline fairings and aft attach structures, core stage repressurization lines, and feedline and repressurization brackets. The ICPS saw approximately 18" of tank stretch in this configuration update that was not incorporated, as this corresponds to less than half an

inch model scale. Figure 1 provides the general configuration arrangements, and Figure 2 shows photographs of the primary model configurations in the tunnel.

The NESC alternate booster nose shapes[2] are shown in Fig. 3. These consist of a canted nose, large radii, canted large radii, ogive, and canted ogive. The AMO and BMO add-on components consisted of several flow fences and replacement fairings for the forward SRB attach structure. In the first campaign, the flow fences were bolted to the core on either side of the SRB forward attach hardware and varied in length, height, and position forward and aft of the attach point station. All were perpendicular to the model surface. As the degree of effectiveness of each design was unknown prior to testing, each BMO configuration was tested at a limited Mach and α range in the TWT to determine which size and position worked best at reducing buffet forcing functions. To save on tunnel resources, only the best performer was tested in the SWT. During the second test campaign, further fence designs were tested, with additional variation in length, height, forward facing edge tapers, radial offset from the forward attach point, and angle with respect to the model surface. Booster mounted fences were also tested. Several forward attach hardware fairings were tested, both alone and in concert with flow fences. Only the two best performing variations were carried forward to the SWT for full Mach regime testing. These were a booster mounted fence with no fairing, and a core mounted fence with no fairing. This last fence was nearly the same as the best from the first campaign, except that the fences were canted inward towards the booster rather than perpendicular to the core OML. Several configurations tested can be seen in Fig. 4.

The models were designed to facilitate model changes in the tunnel. Because the SLS-10003 and SLS-27000 vehicles are identical aft of the forward end of the LOX forward skirt, both 2.5% full stack models utilized the same core and booster stages (Fig. 5a). To make the model change from Block 1 to Block 1B cargo, the LVSA panels were removed and the forebody instrumentation disconnected, which allowed the Block 1 forebody (Fig. 5b) to be removed. The Block 1B forebody (Fig. 5c), made up of the payload fairing and EUS, could then be bolted in place at the LOX forward skirt, its instrumentation connected, and skins bolted closed. A similar arrangement was made for the 4% Block 1 to Block 1B crew configurations. The SLS-10003 and SLS-28000 vehicles share an identical MPCV and LOX forward skirt and LOX tank (Fig. 6a). To make the model change, the LVSA, ICPS, and MSA panels were removed and forebody instrumentation disconnected. The forebody was removed from the common LOX forward skirt, and the common MPCV (Fig. 6c) removed from the MSA. A sting extension (Fig. 6b) to support the EUS and USA could then be bolted to the LOX forward skirt, and the common MPCV bolted to the sting. Adding skins for the EUS and USA completed the model change. Instrumentation was designed to allow for quick disconnects for static and dynamic pressure measurements in these changeable sections.

The model was designed by Donald Morr of Millennium Engineering and Integration Company located at NASA ARC, based on the MSFC-provided computer aided design files of the full scale vehicle. Fabrication and transducer installation were performed by MicroCraft, Inc., in Tullahoma, TN. The NESC nose shapes[2] were fabricated and instrumented at ARC, except for canted ogive, which was manufactured by Langley Research Center (LaRC). The fences, fairings, and SRB field joint rings were also provided by ARC.

The model skins were fabricated primarily of 6061-T6 aluminum and assembled about a series of wagon wheel internal structure anchored to the sting(s), as seen in Fig. 5 – 6. Stainless steel doublers were used for reinforcement along the seams. The LAS tower was fabricated from 17-4 Ph stainless steel. The LAS nose tip of the 4% models, which contained the FADS pressure instrumentation, was brass. The vehicle nose tips were hard anodized to avoid pitting from particulates in the flow. All aerodynamically significant protuberances and excrescences were represented. The protuberances on each respective major component are summarized in Table 1 and depicted in Fig. 7 – 8. The field joint rings and forward booster separation motors (BSMs) can be seen installed in Fig. 4c, Generally, changes in the vehicle OML or specific protuberance pieces that were smaller than two inches full scale (with the 2.5%-scale versions), or one inch full scale (4%-scale versions) were not modeled. Many of the protuberances were developed using additive manufacturing processes of either stereo lithography polycarbonate resin or direct metal laser sintering consisting of aluminum alloy. The core engines and SRB nozzles were not modeled for this test.

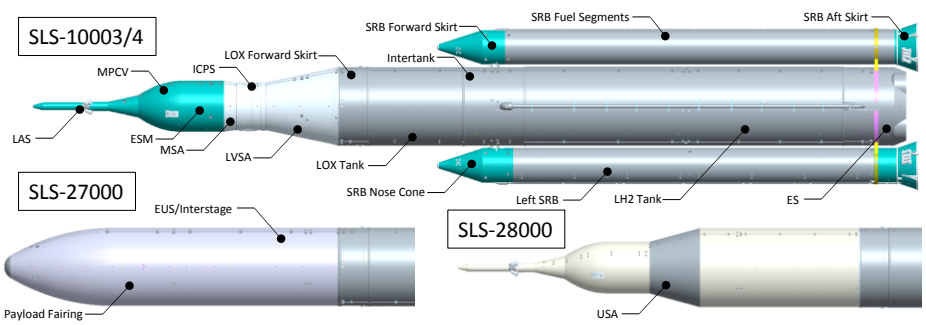

Figure 1. SLS AAT model configurations.

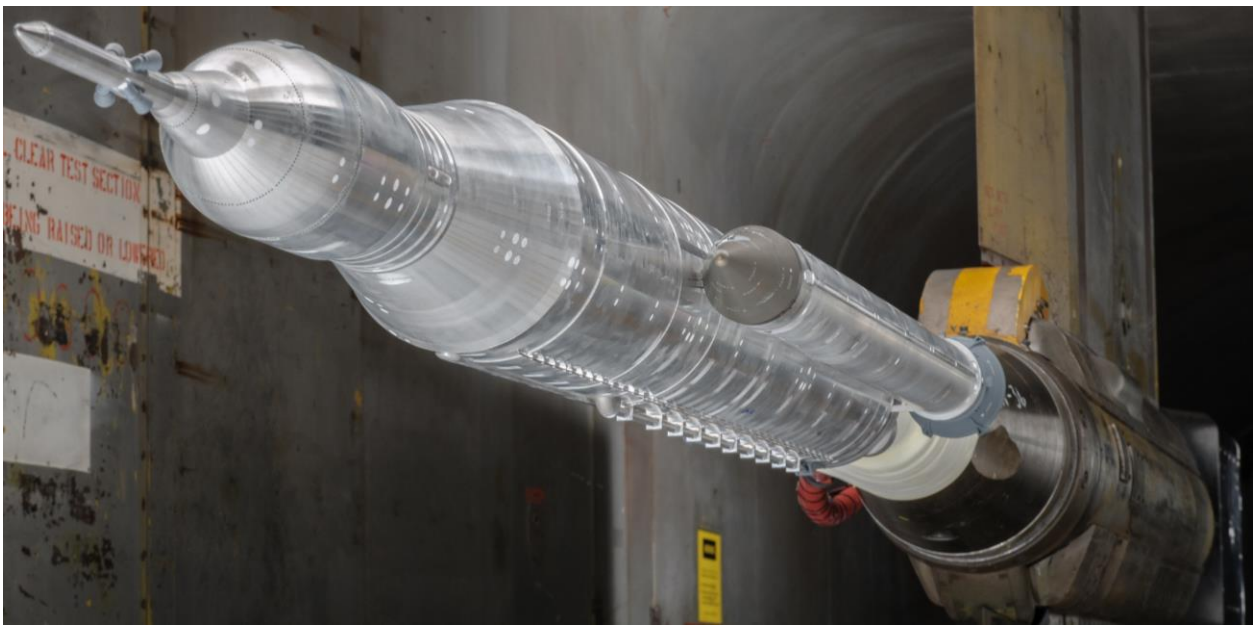

a) SLS 2.5% Block 1 model


b) SLS 2.5% Block 1B cargo model


c) SLS 4% Block 1 model d) SLS 4% Block 1B crew model

Figure 2. SLS AAT baseline models.

a) Baseline nose b) Canted nose c) Large radii nose

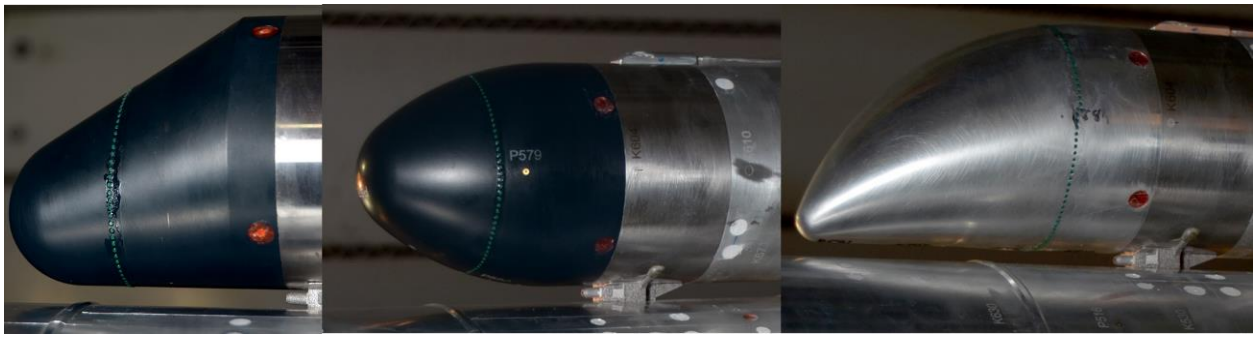

d) Canted large radii nose e) Ogive nose f) Canted ogive nose

Figure 3. SLS AAT NESC sponsored nose shape concepts.

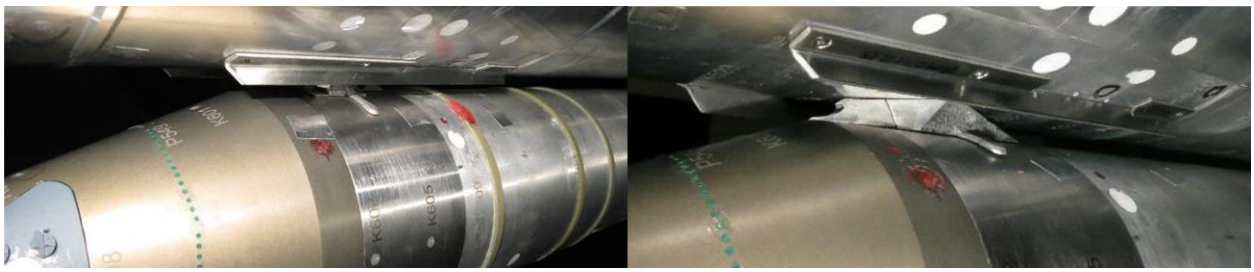

a) Core mounted fences b) Tapered forward attach fairing (with or without fences)

c) Booster mounted fences d) Forward attach fairing (with or without fences)

Figure 4. SLS AAT AMO and BMO fence and fairing examples.

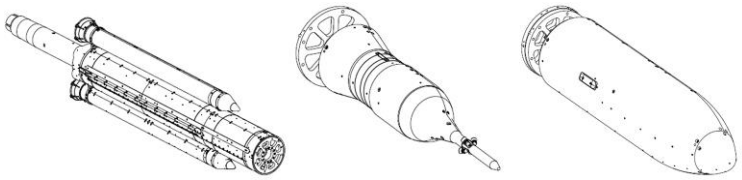

a) Common b) Block 1 crew c) Block 1B cargo

Figure 5. SLS AAT 2.5% model subassemblies.

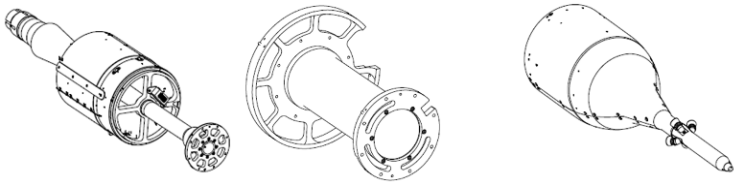

a) Common sting b) Block 1B extension c) Common MPCV

Figure 6. SLS AAT 4% model subassemblies.

Table 1. Protuberances represented on the SLS AAT models.

Vehicle Element	2.5% Full Stack	4% Forebody
Core Stage	Systems Tunnel (1) LOX Feedline and Fairing (2) LOX Aft Attach Structure (2) LOX Repressurization Line (1) LH2 Repressurization Line (1) LOX Forward Skirt Cameras (2) LOX Feedline Brackets (10 per) LOX/LH2 Repressurization Lines (23) LOX/LH2 Repressurization Line Brackets (13 LOX only/23 dual LOX/LH2) Core Engine Fairings (4)	Systems Tunnel (1, truncated) Vehicle Stabilization System Brackets (2) LOX Forward Skirt Cameras (2) LOX Repressurization Line (1, truncated)
Upper Stage	LAS Tower (1) LAS Nozzles (4) MPCV Umbilical (1) Upper Stage Systems Tunnel (2 on ICPS, 1 on EUS)	LAS Tower (1) LAS Nozzles (4) MPCV Umbilical (1) Upper Stage Systems Tunnel (2 on ICPS, 1 on EUS)
SRB (per each)	Systems Tunnel (1) Rooster Tail (1) Hold Down Posts (4) Thrust Vector Control Brackets (2) Kick Ring (1) Booster Attach Ring (1) Forward Attach Hardware (1) Aft Attach Hardware (1) Forward Booster Separation Motors (4) Aft Booster Separation Motors Field Joint Rings (3)*	–

*Only used on left booster during second test campaign.

a) Φ_{sc} = 180° common

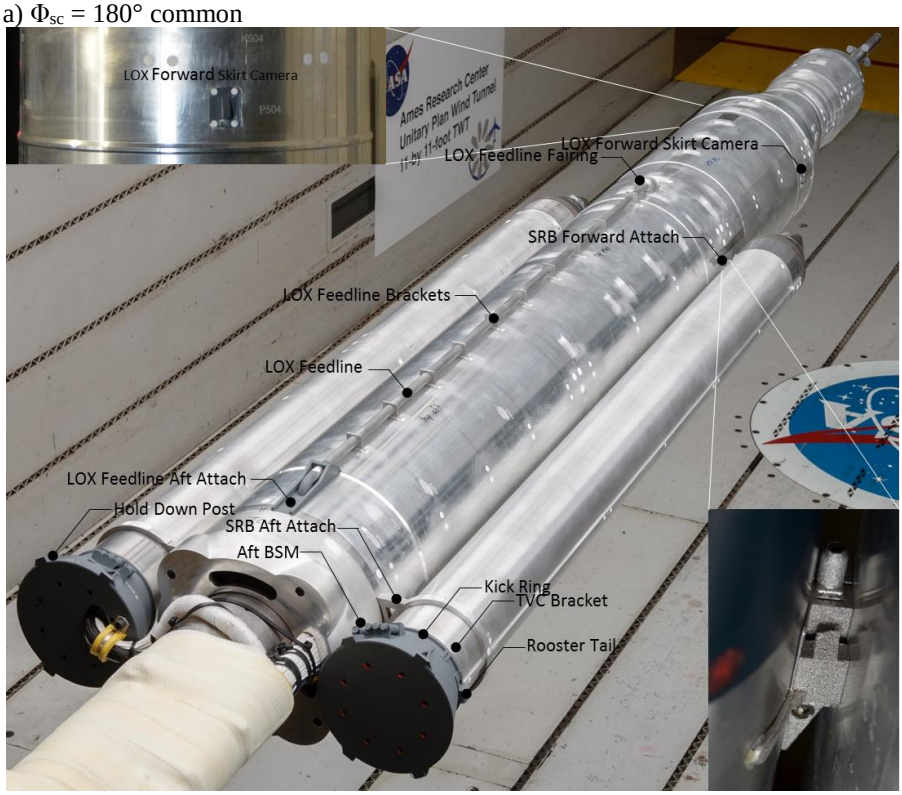

b) Φ_{sc} = 0° common

c) Block 1 d) Block 1B cargo

Figure 7. Common 2.5% core and booster protuberances.

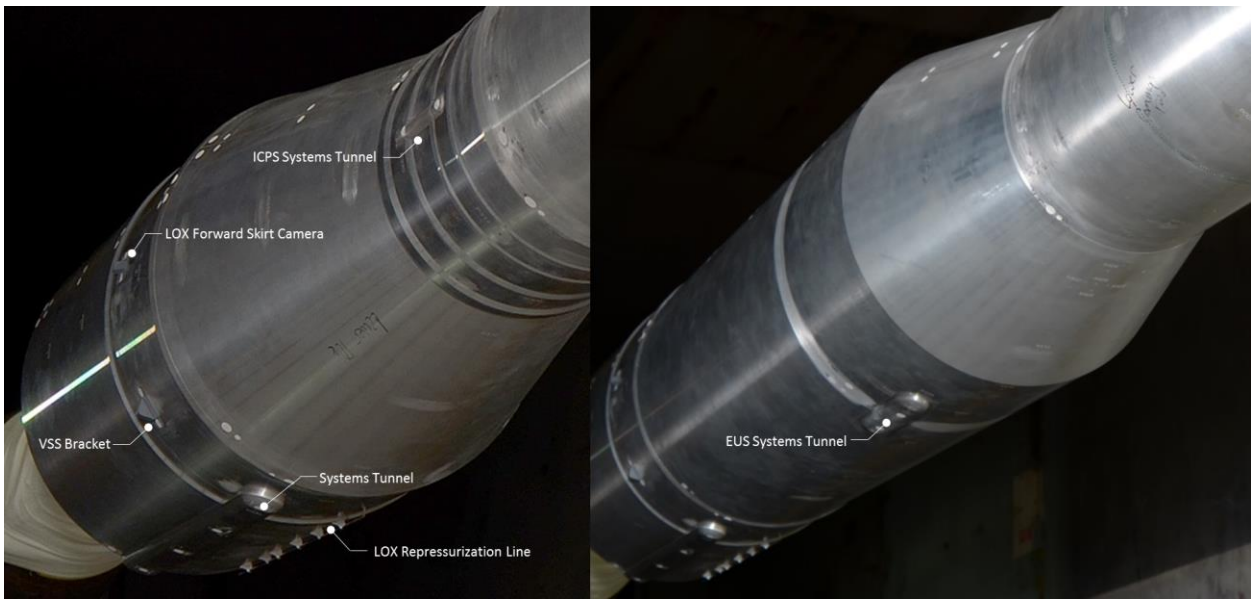

a) Block 1 b) Block 1B crew

Figure 8. Common and Block 1 4% protuberances.

III. Instrumentation

The models were instrumented with high frequency pressure transducers and static pressure taps. Planar projections of all the vehicles are given in Fig. 9 – 10, which depict relative proximity to the protuberances represented by approximate block shapes. The structural coordinate system clocking angle (Φ_{sc}) is shown.

Table 2. SLS AAT Instrumentation Allocation.

Model	Dynamic Transducers	Static Measurements
SLS-10003, 2.5%	161*	39
SRB, 2.5%	60†	23‡
SLS-27000, 2.5%	177	60
SLS-10003, 4%	65	62 + 9 FADS
SLS-28000, 4%	80	58 + 9 FADS

*Two transducers were added to the intertank for the second test campaign, using the channels from two LOX forward skirt transducers

†for SRB Baseline, 59 for NESC Noses (Fig. 2a, 2c, 2e)
57 for NESC Noses (Fig. 2b, 2d)

‡for SRB Baseline, 13 for NESC Noses

A. High Frequency Pressure Transducers

The models were instrumented with a total of 386 unsteady Kulite® Semiconductor Inc. ultraminiature transducers. Models XCL-072-5D and -15D differential transducers were used for aeroacoustic data. To minimize broadband noise induced by the transducer being out of flush with the model OML[6], the transducers were installed via holders. The holders were individually contoured to the model surface prior to transducer installation to ensure flush mounting. The majority of the holders were based on a Kulite B-screen design, consisting of ten equally spaced 0.008 in. diameter holes in a 0.048 in. diameter circle, as shown in Fig. 11. This design has been shown to minimize cavity noise induced by holders used in past NASA testing[7]. The holes were created via laser drilling. In order to support the Buffet Loads Mitigation Task Team formed as a result of SRB forward attach induced buffet loads[3], additional instrumentation was required after B-screen holder assembly was completed. To avoid fabrication delays, these additional transducers were installed using a simpler holder design. This simplified holder consisted of a single 0.048 in. diameter hole in the holder face, as shown in Fig. 12. Table 2 provides transducer number breakdowns by model configuration. In Fig. 9 – 10, B-screen holder transducers are shown in red, and single-hole holder transducers are shown in green.

These models also included five cross-correlation patches. These consisted of five closely spaced transducers arranged in a cruciform and were intended for collection of cross-correlation data should it be required. One was located on the 2.5% ES, one on the Block 1B payload fairing, one on the 4% Block 1 LVSA, one on the Block 1B crew USA, and one on the 4% LOX forward skirt.

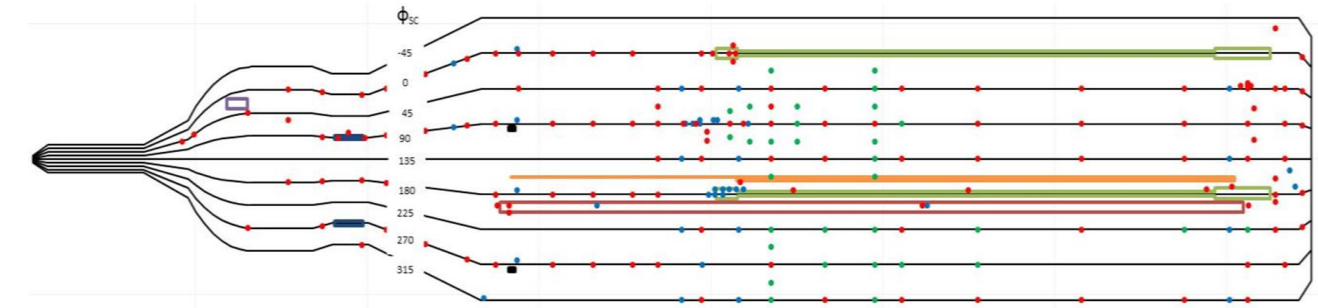

a) SLS Block 1 core configuration

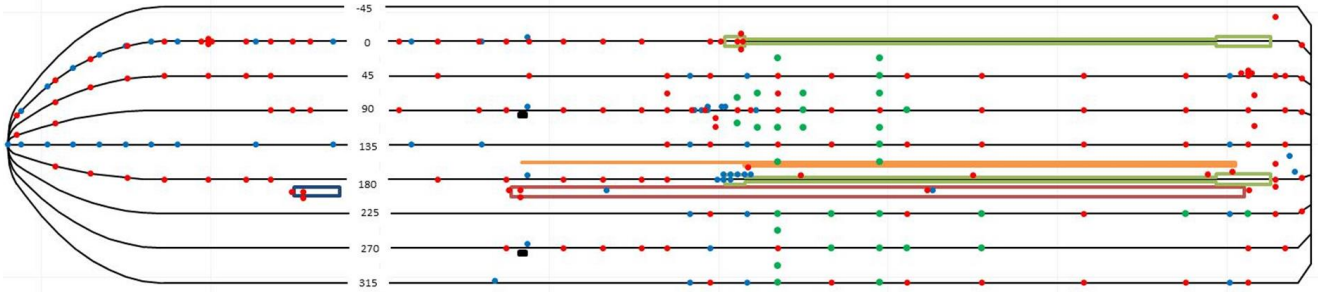

b) SLS Block 1B cargo core configuration

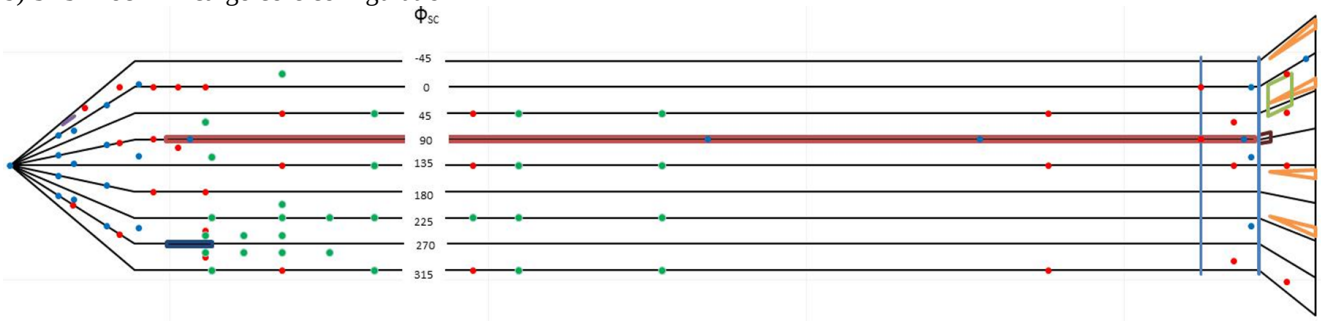

c) SLS Block 1 and Block 1B Left Hand SRB

Figure 9. SLS AAT 2.5% model instrumentation.

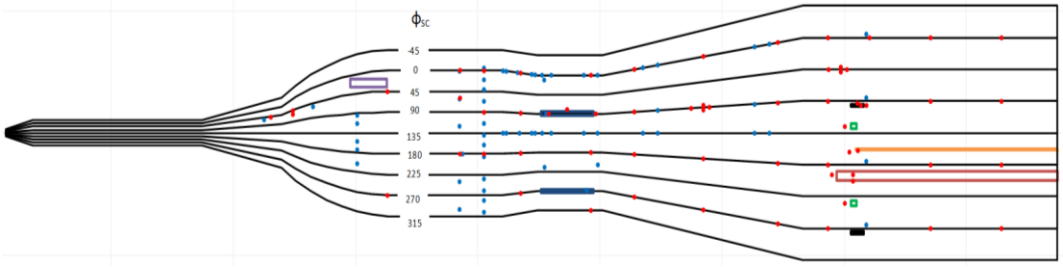

a) SLS Block 1 configuration

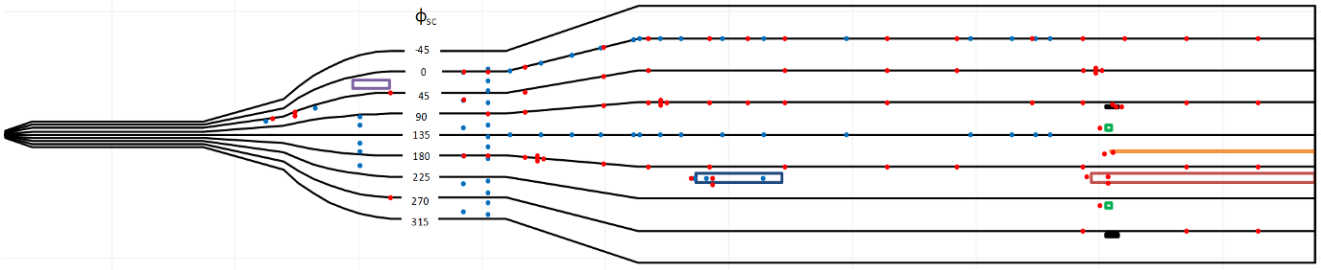

b) SLS Block 1B crewed configuration

Figure 10. SLS AAT 4% model instrumentation.

For the AAT, 350 new transducers were acquired, including 25 spares to account for the approximately 10% attrition rate experienced in recent NASA unsteady aerodynamic tests. This acquisition became insufficient with the additional measurements required for buffet loads mitigation studies. Because transducer acquisition lead-time was approximately nine months at the time of this test, satisfying these additional locations could not be accomplished with new transducers without test delay. The supplemental transducers were therefore salvaged from an Ares I ascent model previously tested at ARC[8]. All measurements on the 2.5% vehicles were populated using new transducers. Cable length for each location was determined using distance from the transducer to either the base of the vehicle or the base of the separation plane for model change-outs. The pressure range was determined based on CFD analysis, experience, and engineering judgment. Seven new transducers were held as spares in the event that in-situ replacement would be required. Three of these were 15 psid transducers (XCL-18-072-15D), and four were 5 psid transducers (XCL-18-072-5D). Note that the test actually experienced a loss of only five transducers, which is well below the expected attrition rate.

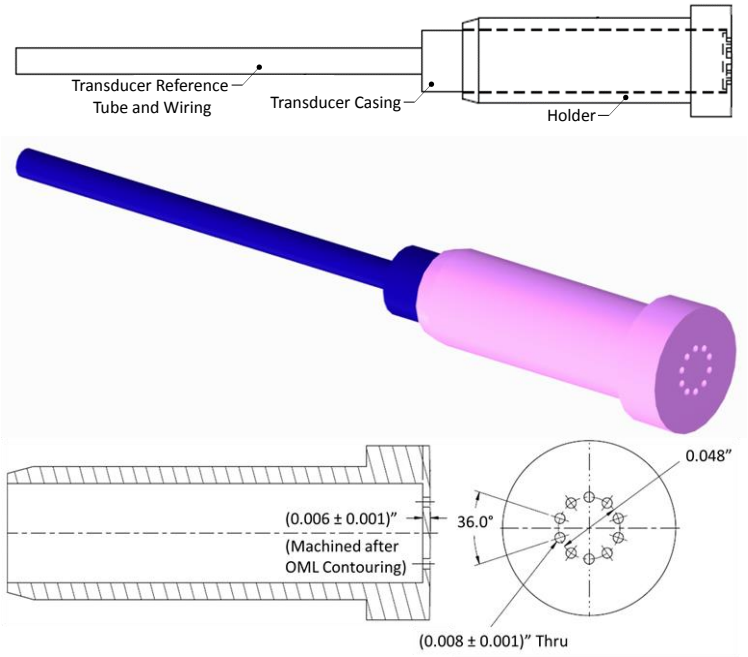

Figure 11. B-screen transducer holder used during SLS AAT for most dynamic measurements.

Most of the Ares salvaged transducers were placed on the SLS-28000 model because it was the lowest priority at the time of testing. However, some transducers on that model were new to protect against the risk of using the salvaged transducers. These new transducers were placed primarily in the areas of greatest interest, particularly on the SLS-28000 USA. The cross-correlation patches on the SLS-28000 vehicle also used new transducers so that phase matching could be ensured. The remainder of the salvaged Ares transducers were used on the remaining 4% model parts (both those unique to the SLS-10003 configuration, and those common to both). These were placed in locations that corresponded to redundant measurements on the 2.5% SLS-10003 model to protect against the risk of using the salvaged transducers. All transducers were provided by MSFC and included individual temperature compensation modules and Omnetics Part No. A12406-001 connectors already attached.

Amplifiers custom-built by ARC provided excitation, amplification, and line driving capability for each transducer. The eight channel amplifiers were located in the strut with approximately 25' of cable between the transducers and amplifiers. The amplified signals were then transmitted to the control room for digitalization via institutional wiring with an approximate length of 125'. Each channel provided ±5.00 V DC excitation and has an approximately 50x linear gain. Individual channel gains were calculated from measured excitation and swept sine transfer function amplitudes from 10 Hz to $100x10^3$ Hz. Amplifiers were

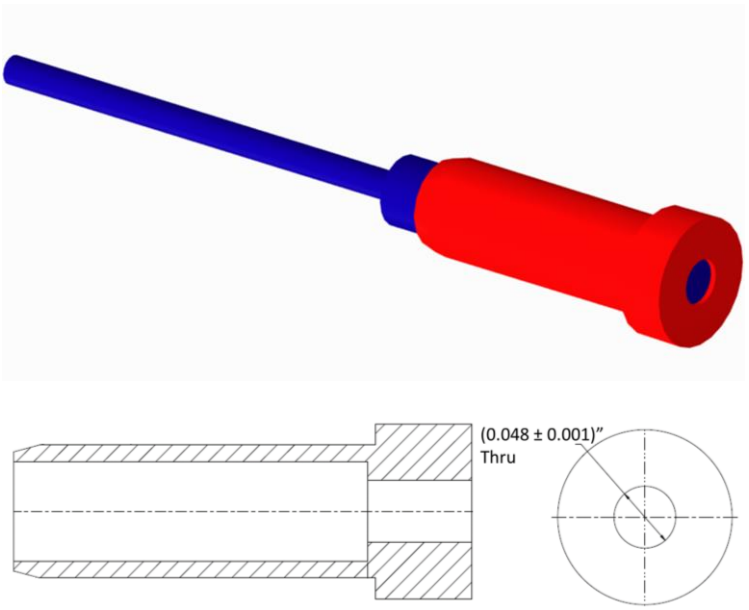

Figure 12. Single-hole transducer holder used during SLS AAT for additional dynamic measurements.

powered by Agilent triple-output power supplies of type E3531A. Each power supply provided ±15 V DC power for two amplifiers. Power supplies were located in the control room. The transducers within each correlation group were connected to a single data acquisition board to minimize cross channel delays.

Each fluctuating pressure transducer included a static pressure tube which was routed to manifolds on-board the model. The manifolds had a controlled pressure set to approximately the test section static pressure.

B. Static Pressure Taps

The models were instrumented with a variable number of static pressure taps, which are illustrated in Fig. 9 – 10 in blue. The static pressures were collected by quarter-hard stainless steel tubing installed using flush-mounted holders that were surface contoured to the model OML. The static tubing was installed with sufficient length to attach flexible tubing connectors to one of two 64-channel, 15 psid electronically scanned pressure (ESP) transducer modules located on-board and provided by ARC. Four ports on each module were plumbed to a regulated known pressure source as a verification check. A variation greater than 2 psf between the verification ports and the regulated source would warrant a re-zero. This value was not exceeded during testing. The ESP modules incorporated digital temperature compensation such that a thermocouple was not required to monitor temperature. Table 2 provides static pressure tap breakdowns by model configuration.

IV. Facility Information

The UPWT at ARC are a set of three interconnected tunnels that share a central main drive system that can be used to drive either a transonic leg (11’ x 11’ TWT) or a supersonic leg (9’ x 7’ SWT), as shown in Fig. 13[9]. The third high speed leg is the supersonic 8’x7’ test section, which is in mothball status and cannot currently be utilized.

The TWT is a closed-return variable-density tunnel with a fixed geometry, ventilated test section, and a dual-jack flexible nozzle. The test section has 5.6% porosity consisting of evenly distributed slots on all four walls. Air flow is produced by a three-stage, axial-flow compressor powered by four wound-rotor variable-speed induction motors. The Mach number range is 0.20 to 1.50 with Reynolds number varying from 0.3- to 9.6-million per foot.

The SWT is also a closed-return variable-density tunnel, but is equipped with an asymmetric sliding block nozzle. The test section Mach number can be varied by translating the fixed contour block that forms the floor of the nozzle in the stream-wise direction. Airflow is produced by an 11-stage, axial-flow compressor powered by the same four wound-rotor variable-speed induction motors used for the TWT. The Mach number range is 1.54 to 2.56 with Reynolds number variation from 0.9- to 6.5-million per foot.

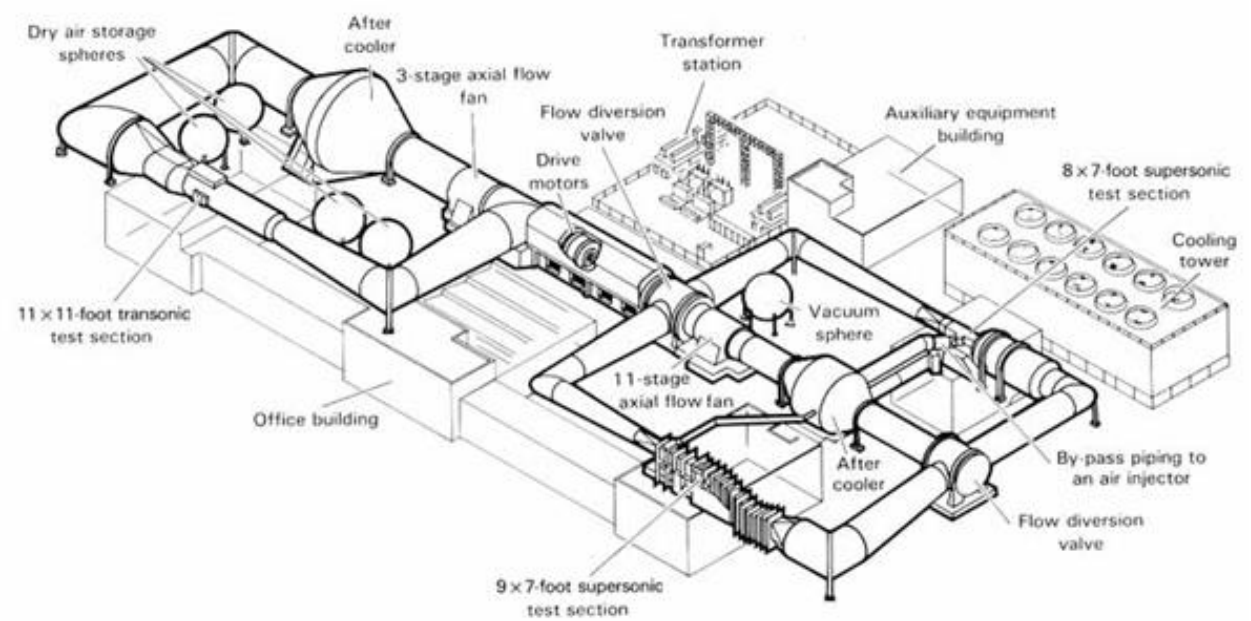

Figure 13. ARC UPWT Layout[9].

V. Operations

A. Calibration and Health Checks

Transducer health checks and phase-matching were performed by ARC. No static calibrations were performed on the unsteady pressure transducers. All static health checks and data processing used factory-supplied calibration for each transducer.

All transducers underwent a static health check that included twelve calibration pressures. For each calibration point a known pressure was applied to the measurement side of the diaphragm. This procedure was performed in a laboratory setting with groups of eight transducers.

Static health checks were also performed several times during the test. During in-situ static health checks, the reference pressure was set to several known pressures. Results of the in-situ static health checks were tracked to document transducer health. Transducers that showed output variation of more than 0.5 decibels (dB referenced to $20x10^{-6}$ pascals) and of more than 1.0 dB were noted as a bad static health check. Repeated cases of greater than 1.0 dB indicate a damaged transducer. Also, to verify the health, operation, and validity of the static pressure modules and the dynamic transducers, measurements were taken with no flow at tunnel pressure conditions after the tunnel was sealed and before the tunnel was opened.

Planned data analysis included correlation processing between select transducers to assess the spatial correlation of the aeroacoustic environment. To maximize the effectiveness of these measurements, transducers with closely matched phase were selected. Phase measurements were made by placing each transducer in a flat plate with an electro-static speaker oriented at a 45° angle to the plate. A pseudo-random maximum length sequence was used to provide a repeatable excitation signal for the transducer under test. A frequency response function of the transducer output and the electro-static speaker input provided amplitude and phase response over the frequencies of interest. Transducers with similar phase response were chosen for the correlation measurement locations.

B. Installation

The 2.5%-scale SLS-10003 full-stack model was initially installed in the TWT. The modified ARC sting SR-55 was the primary model support for the 2.5% models and utilized hub wagon wheel assemblies built for these models. The upper stages of the models were changed out to accommodate the two 2.5% configurations. The NESC booster nose shape changes and BMO and AMO fences also occurred with these models in the TWT.

The modified SR-70 sting with the SR-163 20” extension was utilized for the 4% models. A similar change-out of the payload section was performed between the two model configurations by removing the appropriate skins and leaving the LAS/MPCV unchanged.

Separate model leveling fixtures were included for both model scales to provide alignment in the test units. The models were positioned in the TWT such that the top (defined by the structural and body axes at clocking angle of 0°) was aligned in the vertical plane towards the tunnel ceiling. The pitch center of rotation and vertical height in the test section were adjusted such that interference from the window frames was minimized in the shadowgraph viewing area.

Installation of the test articles in the SWT was accomplished with the same sting hardware items described above, except that the 20” extension was not used with the 4% models. The model top was oriented in the horizontal plane toward the North sidewall of the tunnel which is the left sidewall when viewed from aft.

All plumbing and wiring requirements for the dynamic pressure transducers and the ESP modules were routed out the back of the models and externally to the sting (visible in Fig. 7). Exposed leads were wrapped with Zim-Flex®. The dynamic data system components were transferred between test units and control rooms as needed during transition from the TWT to the SWT as only one system was available.

All models used boundary layer trip devices. Forest green trip dots 0.008” high were used. The dots were typically 0.050” diameter on 0.10” centers. The models with the LAS/MPCV had boundary layer trip devices applied in circular bands at four axial locations from the nose tip. These corresponded to the back of the LAS tower forward cone, the front of the LAS tower aft cone, the midpoint of the MPCV ogive blast protection cover, and on the ESM panels just aft of the MPCV umbilical. These are seen in Fig. 2a, 2c, 2d, and 7c. Due to an anomaly seen in the shadowgraph images during 4% SLS-10003 testing in the TWT, the third trip dot row was removed after completing the scheduled testing. After removal, the 4% SLS-10003 model was re-run at Mach 0.95, 1.1, and 1.2. This third row of trip dots was not in place for the remainder of testing and so is not in place for any 4% SLS-28000 testing. The absence of this row of trip dots is evident in Fig. 2d.

The payload shroud of the SLS-27000 configuration had the same size trip dots, but applied in a single band at the ogive-cylinder juncture. This row is shown in Fig. 2b and 7d. Trip dots were also applied to the SRBs forward of the cone-cylinder juncture, as shown in Fig. 2a, 2b, 3, and 4.

C. Test Operations

Tests of the SLS model configurations consisted of a series of pitch or yaw polars in the TWT and the SWT. The model was pitched and/or yawed to discrete angles, $\alpha, \beta = [0°, \pm1°, \pm2°, \pm2.83°, \pm4°, \pm6°]$. Full α/β data were collected at Mach = [0.7, 0.8, 0.85, 0.9, 0.95, 1.05, 1.10, 1.20, 1.40, 1.55, 1.75, 2.00, 2.25, and 2.50]. Additionally, Mach sweeps were performed at $\alpha, \beta = 0°$ to investigate potential transient shocks. In the TWT, the Mach increment was 0.01 from 0.85 up to 1.40. A Mach increment of 0.02 was used in the SWT from 1.55 through 2.00. Sweeps were only run using the SLS Block 1 full stack baseline. Data were only obtained once the conditions had stabilized within specified residual tolerances. Residual tolerances used are given in Table 3.

Simultaneous acquisition across all dynamic channels was accomplished using National Instruments PXI based hardware and several computers running Windows® XP. All collection computers were connected to PXI-1045 chassis via MXI-2 PXI-8360 interface cards. The data system coordinator (DSC) used seven PXI-6652 timing and routing cards. One PXI-6652 card generated the master acquisition clock and triggers, and the other six distributed the signals to each of the acquisition chassis. Data acquisition was triggered by the DSC computer when the wind tunnel systems indicated that freestream and model position conditions were achieved, as in Table 3. Data acquisition triggers were received by the PXI 6652 timing cards located in each of the acquisition chassis. Data were digitized using PXI 4462 24-bit A/D cards capable of $204x10^3$ samples per second.

To maximize bandwidth of measured data and to minimize storage requirements, data were split into a high and low rate data files. Data were initially sampled at a high rate for a long duration to satisfy frequency

Table 3. Residual Tolerances for Stabilized Tunnel Condition

Variable	Tolerance
Mach	±0.005
Total Pressure	±5 psf
Total Temperature	±5° Rankine
Reynolds Number	$\pm5x10^4$ 1/foot
Pitch/Yaw	±0.25°

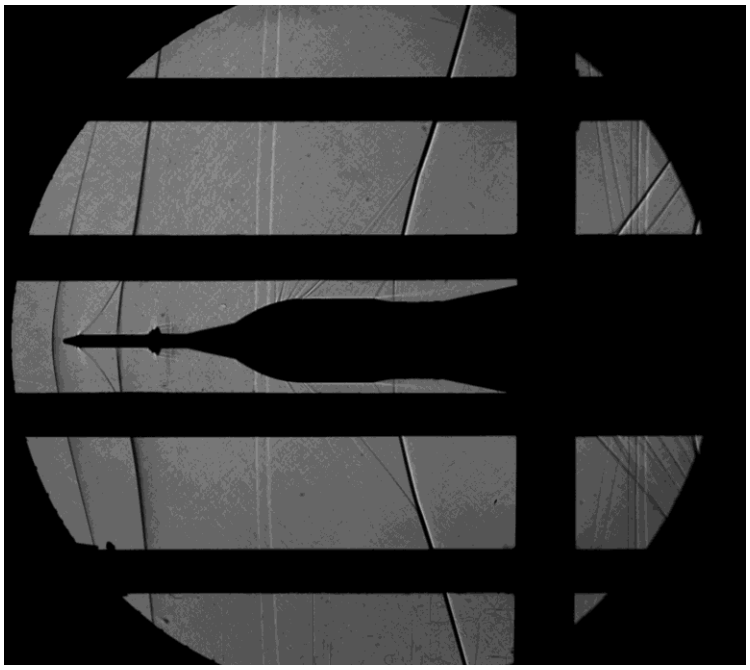

a) TWT shadowgraph during the first test campaign

b) TWT shadowgraph during the second test campaign

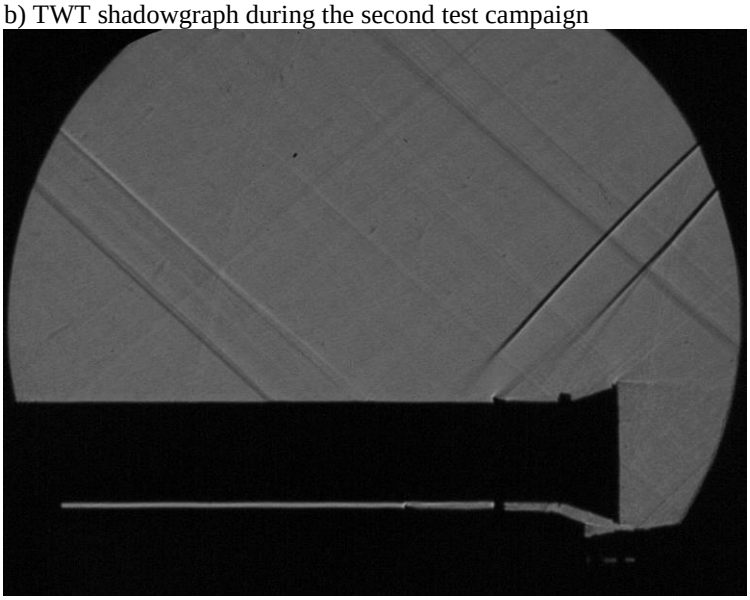

c) SWT shadowgraph

Figure 14. Shadowgraph samples.

requirements. As data were moved to the dynamic data server, each acquisition computer truncated the data set to provide the high rate data and decimated the data set after performing a low-pass filter operation to provide long duration low frequency data. Dynamic data sampling rates for the 2.5% models were generally 153.6 kHz for high frequency and 9.6 kHz for low frequency (~2.7 seconds and ~22 seconds duration, respectively). Dynamic data sampling rates for the 4% models were generally 102.4 kHz and 6.4 kHz (~4 seconds and ~11.5 seconds duration, respectively). Data sampling rate for the static system was 100 Hz for five seconds. Sequencing and acquisition between the static data, dynamic data, optics, and model attitude control systems were accomplished within standard facility practices and were demonstrated during facility checks prior to air-on runs[4].

D. Visualization

Shadowgraph photographs and movies were obtained for the points during pitch polars. The focus during the first test campaign in the TWT was to capture as much of the model as possible from the nose tip towards aft. During the second test campaign, the objective was to capture detail in the SRB forward attach/core intertank region. The model was rolled 90° to accomplish this. Testing in the SWT required the viewing window to be positioned in the aft location for the purpose of observing shock reflection impingement on the aft end of the models. The small optical window was rotated in the steel blank on occasion for optimal coverage in the rear window of the SWT. Samples are shown in Fig 14.

In addition, retro-reflective background oriented schlieren (RBOS) was obtained in the TWT during the first campaign to observe the region between the boosters and centerbody. A ceiling mounted Vision Works Phantom v641 high-speed digital camera was used with the speckled reflective background affixed to the floor.

Photographs of the model and installation were obtained. Direct video of all runs was taken through the available viewing ports.

VI. Data Analysis

A. Dynamic Data Analysis

Data processing was done largely using MATLAB®. Data were delivered in the form of pressure time histories in native counts. Data were converted to voltage from the data acquisition system native format and then to engineering units, taking into account amplifier gain using scaling, offset, gain, and calibration coefficients in data acquisition scripts provided by ARC. Because this analysis is concerned only with the fluctuating pressure component of the time history, the static component of the time history data was removed. This was accomplished by detrending, which removes linear trends from a dataset. This process tares the time history data so that pressure data fluctuates about a zero rather than some non-zero static pressure. The data were then Fourier-analyzed to provide power spectral density (PSD) spectra that could be converted to narrowband aeroacoustic spectra using the MATLAB® function pwelch()[10]. This function uses Welch's method, and this analysis utilized a Hanning window, Fast Fourier Transform block size of 4096 for the high rate data and 1024 for the low rate data, a window equal to block size, and zero overlap. All frequencies above a Nyquist cutoff of the sample rate divided by 2.56 were removed from analysis. PSDs were converted to narrowband in dB using Eq. (1), where $L_{p,MS}$ is the model scale narrowband FPL in dB, and P_{ref} is the reference pressure, $20\text{x}10^{-6}$ pascals.

$$L_{p,MS} = 10\log_{10}\left(\frac{\text{PSD} * \text{Sample Rate} / \text{Window}}{P_{ref}^2}\right) \tag{1}$$

Corrections to the data were done in model scale. Tunnel noise was removed using empty tunnel acoustic surveys of the UPWT test sections[11]. Sources of tunnel noise included the compressor, strut, and wall slots in the TWT and compressor in the SWT. High frequency tones due to transducer mount induced noise from the single-hole holder transducers were also removed. Shock reflections off the SWT walls and ceiling were taken into account. Location of OML impingement was estimated per recommendations of the tunnel user guide[9], and all measurements aft of a shock reflection impingement were ignored. Bad runs and measurements were also removed. These points were identified using health checks throughout the test, and also by time history review post-test.

Data were scaled to full scale using the SLS Ascent Aeroacoustic Design Trajectory[12]. Amplitude was scaled assuming the nondimensional FPL coefficient, $\Delta C'_p$, at a given vehicle location in the wind tunnel is equivalent to that at full scale, as in Eq. (2), where p'_{rms} is root-mean-square acoustic pressure and q_∞ is free stream dynamic

pressure. Using the definition of FPL in Eq. (3), amplitude scales as a function of the flight-to-tunnel dynamic pressure ratio, given in Eq. (4).

$$\left|\Delta C_p^{'}\right|_{flight} = \left|\Delta C_p^{'}\right|_{tunnel} \text{ where } \Delta C_p^{'} = {p_{rms}^{'}}/{q_\infty} \tag{2}$$

$$\text{FPL} = 20\log_{10}\left({p'_{rms}}/{P_{ref}}\right) \tag{3}$$

$$\text{FPL}_{flight} = \text{FPL}_{tunnel} + 20\log_{10}\left({q_{\infty,flight}}/{q_{\infty,tunnel}}\right) \tag{4}$$

Frequency was scaled assuming the nondimensional Strouhal number, *St*, in the wind tunnel is equivalent to that at full scale, as in Eq. (5) where *f* is frequency, *l* is a characteristic dimension such as diameter or length, and *U* is flow velocity. Therefore, frequency scales as a function of wind tunnel model scale and flight-to-tunnel velocity. Because the tunnel medium is air, at a given Mach number velocity is only a function of static temperature (*T*) and so frequency scales as in Eq. (6).

$$\left|St\right|_{flight} = \left|St\right|_{tunnel} \text{ where } St = {fl}/{U} \tag{5}$$

$$f_{flight} = \frac{l_{tunnel}}{l_{flight}}\sqrt{\frac{T_{flight}}{T_{tunnel}}}\, f_{tunnel} \tag{6}$$

The resulting full-scale narrowband spectra were integrated to produce one-third octave bands, ranging from 10 to 2000 Hz. Full bandwidth levels below 70 Hz were taken from the low sample rate data, and levels above 70 Hz from the high sample rate data. Full-scale overall FPL (OAFPL) levels were calculated by log summing one-third octave FPLs over the entire bandwidth.

B. Dynamic Data Results

Results from the AAT for the baseline Block 1 and Block 1B configurations are provided here as Fig. 15-24. As current SLS designs call for use of the baseline configurations with standard SRB nose caps and no flow fences, AMO, BMO, and alternate nose cap environments are not fully developed and are not included. Full bandwidth OAFPLs are provided as a function of vehicle station. These consist of maximum of maximum envelopes of all transducers within a zone for all velocity conditions in each tunnel and $\alpha_T \leq 4.47°$. Transducers were grouped into zones based on similar flow field and OML geometry. While OAFPL magnitudes have been removed, the scales of all plots are consistent with each other, with major y-axis increments at 10 dB. Relative levels across all configurations shown can therefore be determined from these plots. For the general acreage environments in Fig. 15 – 19, solid lines correspond to measurements taken away from the influence of the SRBs (or core), while dashed lines correspond to measurements taken in proximity to the SRBs (or core). Protuberance OAFPLs are provided in Fig. 20 – 24.

Much work has been conducted to verify the data coming out of these tests. Within the AAT program itself, comparisons between repeat runs and between the 2.5% and 4% forebody models of the SLS Block 1 vehicle show good agreement. Also, repeat runs between the first and second test campaigns show good agreement. Data have also been compared to co-located transducers from previous SLS unsteady testing run using a 3% model in R-134a gas with higher Reynolds number in the LaRC Transonic Dynamics Tunnel[3]. These comparisons show good agreement. Also, core measurements in proximity to the SRBs are corroborated in frequency and amplitude by testing from the Space Transportation System program, which utilized very similar geometry in these areas[13].

VII. Conclusions

The SLS AAT was a success. All primary and secondary test objectives were accomplished, with only a loss of five transducers throughout testing. One transducer needed replacement during the first test campaign, and this was accomplished while other models were being tested with no impact on schedule. Replacement of three other transducers was performed between the first and second test campaigns.

These data have been used to successfully develop the SLS-10005 Block 1 design environments, as well as the SLS-27004, -27502, and -28004 preliminary environments. Preparation is underway for Exploration Mission 1, the maiden flight of SLS, which will provide co-located flight measurements to further validate these data. Data from these tests are currently being used for venting environment determination, unsteady CFD development, and advancing the understanding of the complex multi-body flow fields around these vehicles.

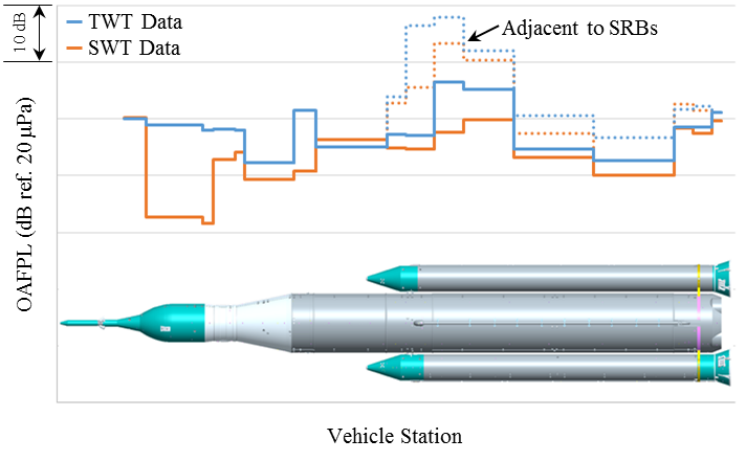

Figure 15. SLS Block 1 OAFPL general acreage environments for payload and core zones.

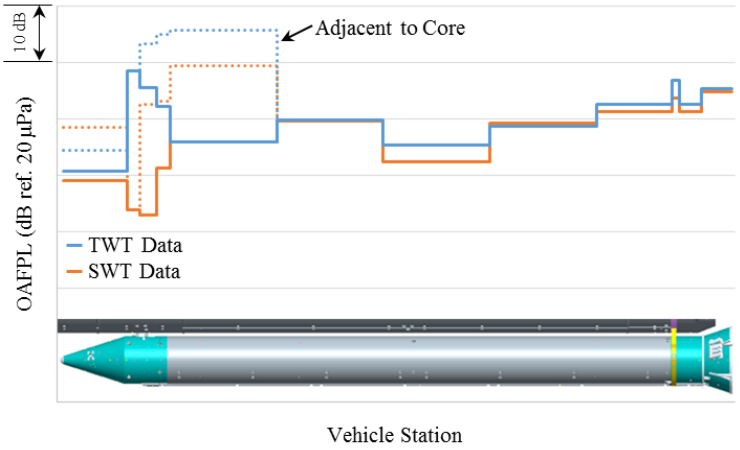

Figure 16. SLS Block 1 OAFPL general acreage environments for booster zones.

Acknowledgments

The authors would like to thank the SLS Ascent Aeroacoustics Test Team for executing a challenging and successful test program. This includes the ARC Fluid Mechanics, Computer Systems and Instrumentation, and Operations Branches. The test also required extra help for in-situ data analysis and measurement health monitoring from both the Aerodynamics and Aerothermodynamics Teams in EV33, as well as the MSFC Fluids Dynamics Branch and the LaRC Aeroelasticity Branch. The authors would also like to thank EV33 and SLS management for support.

References

[1] "Ares I Acoustic Environments Data Book," CxP 72164, 2009.

[2]Bracukmann, G. J., Streett, C. L., Kleb, W. L., Alter, S. J., Murphy, K. J., Glass, C. E., "Computational and Experimental Unsteady Pressures for Alternate SLS Booster Nose Shapes," 53rd AIAA Aerospace Sciences Meeting, January 2014.

[3]Piatak, D. J., Sekula, M. K., Rausch, R., Florance, J. R., Ivanco, T. G., "Overview of the Space Launch System Transonic Buffet Environment Test Program," 53rd AIAA Aerospace Sciences Meeting, January 2014.

[4]Crosby, W. A., Herron, A. J., Reed, D. K., "Ascent Acoustic Tests of the SLS DAC2 Scaled Models in the NASA Ames Research Center Unitary Plan Wind Tunnels," NASA/MSFC EV33-15-016, July 2015.

[5]Crosby, W. A. and Herron, A. J., "Addendum to the Ascent Acoustic Tests of the SLS DAC2 Scaled Models in the NASA Ames Research Center Unitary Plan Wind Tunnels," NASA/MSFC EV33-15-017, July 2015.

[6]Efimtsov, B. M, et. al., "Effect of Transducer Flushness on Measured Surface Pressure Fluctuations in Flight," *43rd AIAA Aerospace Sciences Meeting and Exhibit*, CP 2005-0800, *AIAA Meeting Papers on Disc [CD-ROM]*, Disc 2, AIAA, Reston, VA, 2005.

[7]"Reducing the Effect of Transducer Mount Induced Noise on Aeroacoustic Wind Tunnel Testing Data with a New Transducer Mount Design," Herron, A. J., Reed, D. K., and Nance, D. K., 21st AIAA/CEAS Aeroacoustics Conference, June 2015.

[8]Hamilton, C. R., Mayle, M. N., Crosby, W. A., Nance, D. K., Reed, D. K., "Ascent Acoustics Test of a 4%-Scale Ares I Model in the NASA Ames Research Center Unitary Plan Wind Tunnel," ESTSG-FY09-00450, February 2009.

[9]"Test Planning Guide for High Speed Wind Tunnels," NASA Ames Research Center, Report Number A027-9391-XB2, Revision 5, April 27, 2005.

[10]"pwelch," *MathWorks® Documentation*, URL: http://www.mathworks.com/help/signal/ref/pwelch.html [cited 9 November 2015].

[11]Amaya, M. A., Richey, C. S., "Preliminary Data Transmittal for the 11-ft Acoustics Survey Test (Test Number 11-0196) conducted in the Ames Research Center 11-Ft. TWT," 10 Oct 2008.

[12]Dukeman, G., "Space Launch System Aeroacoustic Design Environment Development," NASA/MSFC EV42-14-004, 19 Sept. 2014.

[13]"Space Shuttle System Acoustics and Shock Data Book," Rockwell International Corporation, Space Division, Report No. SD74-SH-0082B CHG 4, 10 Sept. 1996.

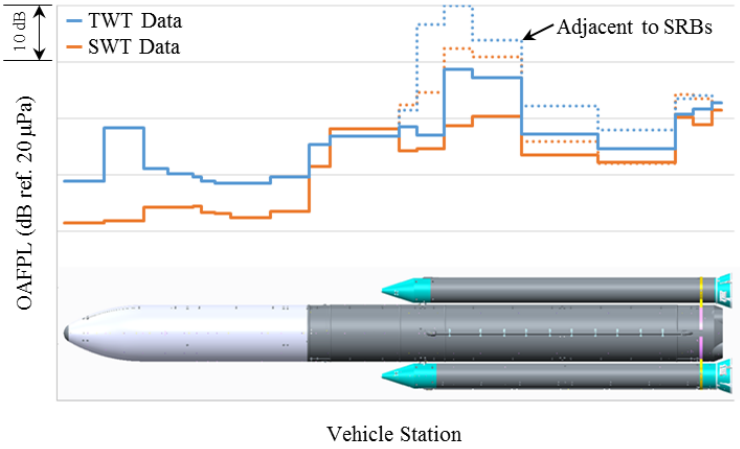

Figure 17. SLS Block 1B cargo OAFPL general acreage environments for payload and core zones.

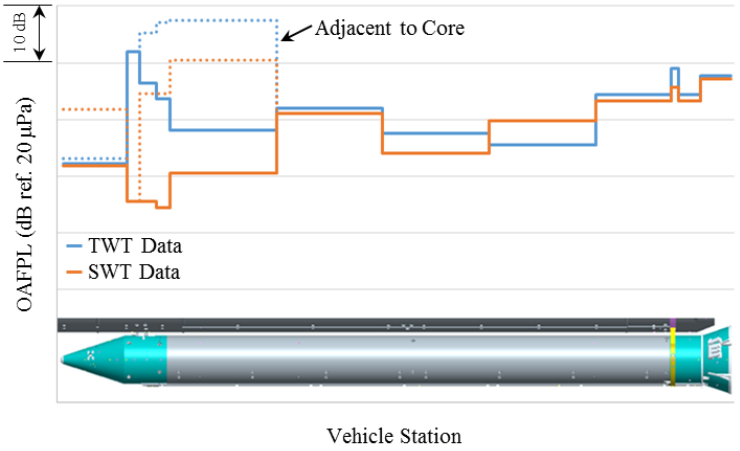

Figure 18. SLS Block 1B cargo OAFPL general acreage environments for booster zones.

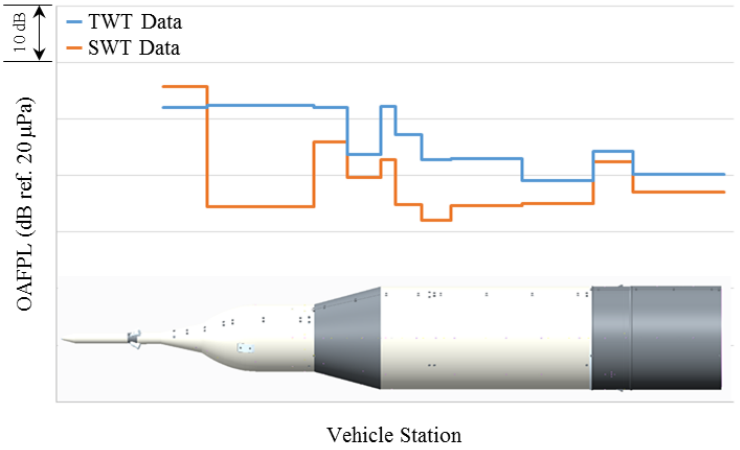

Figure 19. SLS Block 1B crewed OAFPL general acreage environments for payload and core zones.

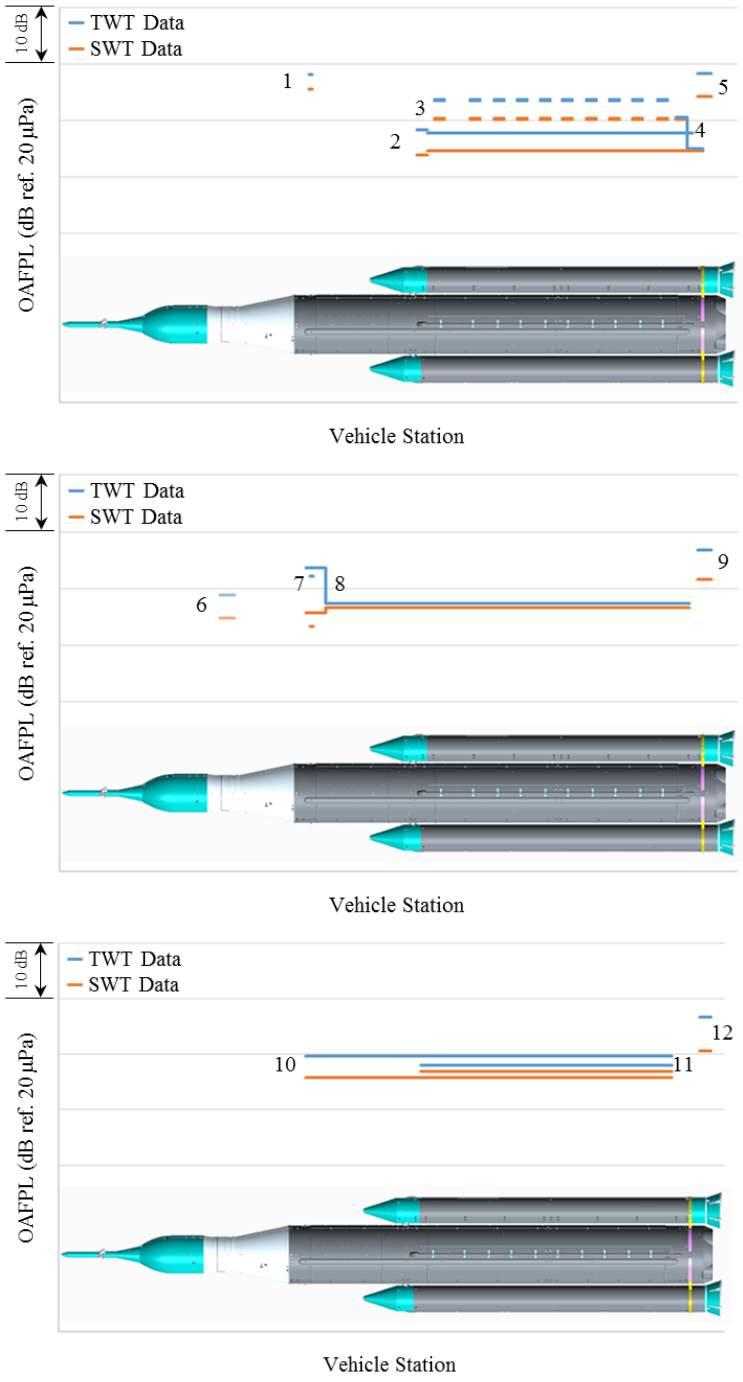

1. VSS Bracket, 2. LOX Feedline and Fairing, 3. LOX Feedline Brackets, 4. LOX Feedline Aft Attach Bracket, 5. Upper and Diagonal SRB Struts, 6. ICPS Systems Tunnel, 7. LOX Forward Skirt Cameras, 8. Systems Tunnel, 9. Lower SRB Strut, 10. LOX Repressurization Line, 11. LH2 Repressurization Line, 12. Engine Fairings

Figure 20. SLS Block 1 OAFPL protuberance environments for payload and core.

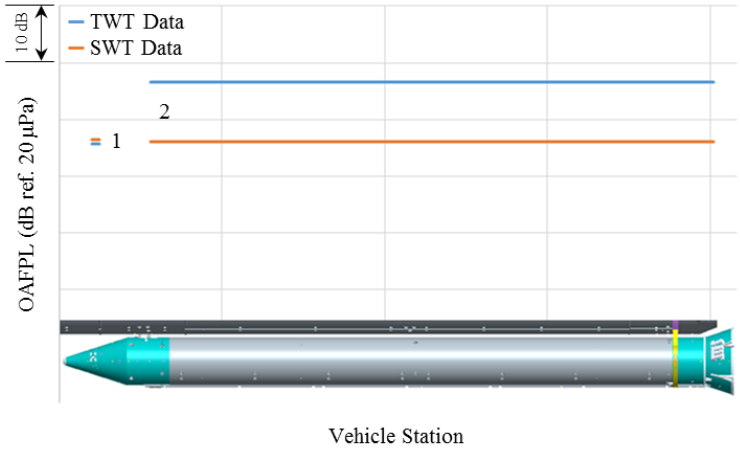

1. Forward BSMs, 2. SRB Systems Tunnel

Figure 21. SLS Block 1 OAFPL protuberance environments for booster.

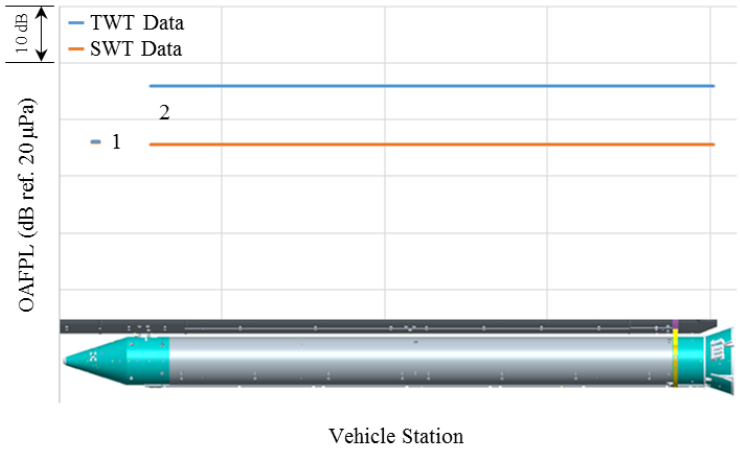

1. Forward BSMs, 2. SRB Systems Tunnel

Figure 22. SLS Block 1B cargo OAFPL protuberance environments for booster.

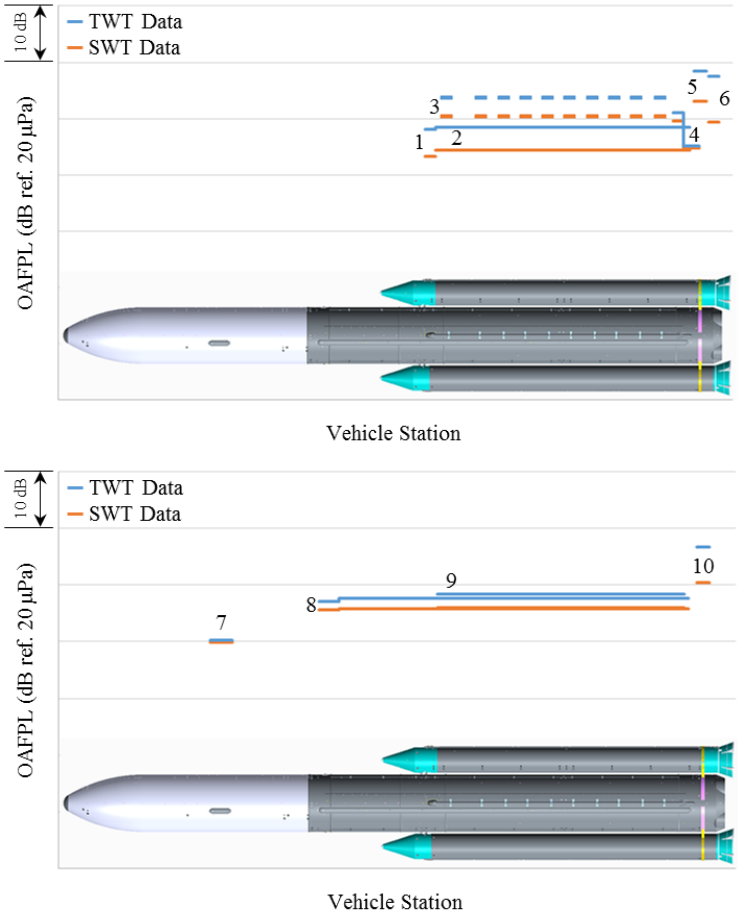

1. LOX Feedline Fairing, 2. LOX Feedline, 3. LOX Feedline Brackets, 4. LOX Feedline Aft Attach Bracket, 5. Upper and Diagonal SRB Struts, 6. Engine Fairings, 7. EUS Systems Tunnel, 8. Systems Tunnel, 9. LH2 Repressurization Line, 10. Lower SRB Strut

Figure 23. SLS Block 1B cargo OAFPL protuberance environments for payload and core.

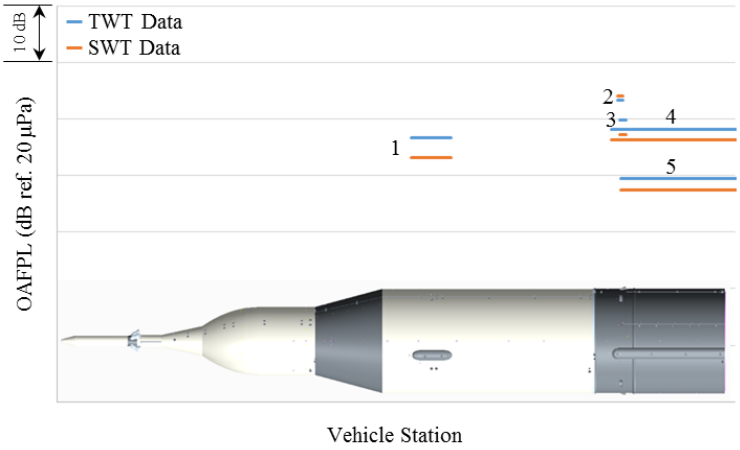

1. EUS Systems Tunnel, 2. VSS Brackets, 3. Forward Skirt Cameras, 4. Systems Tunnel, 5. LOX Repressurization Line

Figure 24. SLS Block 1B crew OAFPL protuberance environments.